Measurements of the mean lifetime and kinetic-energy release of metastable CO^{2+}

J. P. Bouhnik,* I. Gertner, and B. Rosner
Department of Physics, Technion, Haifa, 32000, Israel

Z. Amitay,† O. Heber, and D. Zajfman
Department of Particle Physics, Weizmann Institute of Science, Rehovot, 76100, Israel

E. Y. Sidky and I. Ben-Itzhak‡
J. R. Macdonald Laboratory, Department of Physics, Cardwell Hall, Kansas State University, Manhattan, Kansas 66506

(Received 19 June 2000; published 8 February 2001)

We present a method that allows state-selective measurement of the lifetime of metastable doubly charged molecular ions. The method is based on the simultaneous measurement of kinetic-energy release upon dissociation and lifetime and relies on three-dimensional fragment imaging. The experimental determination of the energy and lifetime of a vibrational state provides a stringent test for the theory. Using this method, we have measured the lifetime of two vibrational states of $^{12}C^{16}O^{2+}$. Explicitly, $\tau = 670 \pm 50$ ns and $\tau = 26 \pm 5$ ns were measured for the states with $E_k = 5.713$ eV and $E_k = 5.841$ eV, respectively. The measured mean lifetimes and kinetic-energy releases are consistent with previous measurements, and the results indicate that further theoretical work is required.

DOI: 10.1103/PhysRevA.63.032509 PACS number(s): 33.70.Ca, 33.80.Gj

I. INTRODUCTION

Doubly charged diatomic ions are unique metastable species with unusual bonding and dissociation properties. These species play an important role in various aspects of gas phase chemistry. Dications exhibit a wide range of lifetimes against dissociation, depending on the decay mechanism and the position of the vibrational-rotational level with respect to the barrier height. Although many doubly charged ions have been investigated by both experimentalists and theorists, comparison between the experimental results and the theory for the lifetimes of these species has been extremely difficult. The main reason is the sensitivity of the lifetime, over many orders of magnitude, to the initial quantum states of the molecule prior to dissociation. As it is difficult to produce molecular ions in a well defined vibrational distribution, different experiments will usually lead to different lifetimes.

Another uncertainty in these measurements is related to the decay mechanism. Even state-selected measurement of the lifetime of doubly charged ions AB^{2+} does not always help to identify the dissociation process. These processes can be classified, in general, under three categories. The first one is related to tunneling through the barrier formed by the avoided crossings between, for example, two adiabatic potential-energy curves corresponding to $A^{2+}+B$ and $A^{+}+B^{+}$. The second category is related to predissociation due to curve mixing or curve crossing, and the last one is the electronic decay from an excited metastable bound state, to a dissociative state. Very often, two or even three decay mechanisms can coexist, and the different branching ratios are usually a strong function of the initial rovibrational state of the molecular ion.

Over the last few years, the mean lifetimes of a variety of doubly charged molecular ions have been measured. Among all, the one that has attracted the largest interest is CO^{2+} [1]. The measured mean lifetimes span a wide range of times from submicroseconds to a few seconds. Newton and Sciamanna [2] and Hirsch *et al.* [3] reported mean lifetimes of 20^{+10}_{-5} and 16^{+1}_{-7} μs, respectively, and a dissociation energy of 5.75 ± 0.02 eV [2]. Mean lifetimes around and somewhat below 1 μs were observed by Dujardin *et al.* [4], by Safvan and Mathur [5] (1.0 ± 0.25 μs), and by Field and Eland [6] (600^{+600}_{-200} ns). In contrast with the single pass experiments mentioned above much longer lifetimes were observed using the storage ring technique [7,8]. Andersen *et al.* [7] reported mean lifetimes of 0.8 and 6 ms with an additional ''stable'' component with a lifetime larger than 3.8 s. Mathur *et al.* [8] reported mean lifetimes of 0.2, 4, and 15 ms, with a couple of ''stable'' components with values of 4 and 8 s. The main reasons for such a wide range of values for the lifetime are the lack of control of the initial quantum state distribution of the CO^{2+} molecular ion, and that each experimental setup is sensitive to a specific range of dissociation times.

Recently, measurements of $^{12}C^{16}O^{2+}$ dissociation with vibrational level resolution have been reported [9–12]. From the spectra of these measurements it is possible, in some cases, to evaluate the lifetime. Both Lundqvist *et al.* [10] and Penent *et al.* [12] measured a mean lifetime of about 0.65 μs associated with the predissociation of the $^1\Sigma^+$ state (see Fig. 1). The advantage of these methods is that the measured lifetimes are associated with well defined

*Present address: ELGEMS, 10 Hayozma St., Tirat Ha'Carmel, Israel.

†Present address: JILA, National Institute of Standards and Technology and University of Colorado, Department of Chemistry and Biochemistry and Department of Physics, University of Colorado, Boulder, CO 80309-0440.

‡Corresponding author. Electronic address: ibi@phys.ksu.edu

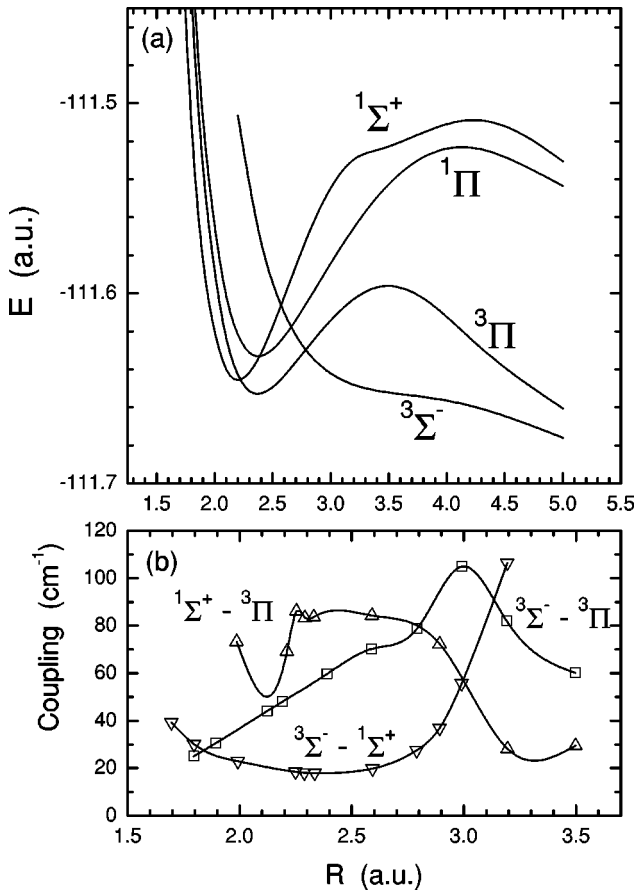

FIG. 1. (a) Potential-energy curves and (b) coupling terms of CO^{2+}, from Andersen *et al.* [7].

initial states so that the results can be directly compared with theoretical calculations.

In the following, we present a method for measuring the lifetime of metastable states of doubly charged molecular ions. The method is state sensitive, and can differentiate between different modes of decay. The dynamic range of the method goes from tens of nanoseconds to a few tens of microseconds. We have chosen to focus on the CO^{2+} molecular ion for this experiment in order to be able to compare our results with both existing theoretical calculations and previous experimental data.

II. DISSOCIATION MECHANISMS AND KINETIC-ENERGY RELEASE

A schematic potential energy curve diagram of a typical doubly charged molecular ion AB^{2+} is shown in Fig. 2, where all three different types of decay mechanism are indicated. Also shown is the kinetic energy released (KER) upon unimolecular dissociation of the doubly charged molecular ion. This KER can be used, at least partially, to characterize the decay mechanism. For example, very narrow distributions are associated with decay by predissociation [denoted (a) in Fig. 2] and tunneling through the potential-energy barrier [(b) in Fig. 2], while a wide distribution is the result of electronic decay to a lower dissociating state [(c) in Fig. 2].

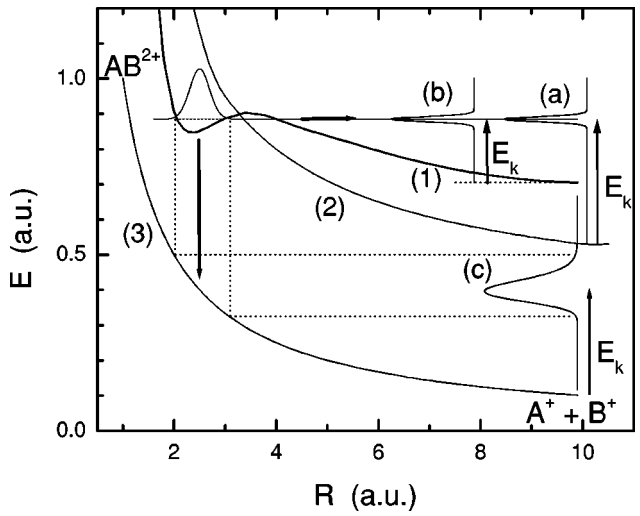

FIG. 2. Schematic potential-energy curves of a typical AB^{2+} molecular ion. Curve (1) supports metastable states while (2) and (3) are repulsive. The decay mechanisms are denoted on the figure as (a) predissociation, (b) tunneling, and (c) dipole transition to a dissociating state.

The large width of the last is due to the distribution of initial internuclear distances described by the vibrational wave function. This broad distribution might have some structure reflecting the shape of the initial distribution $|\psi_v(R)|^2$ if a specific initial state is dominant, otherwise it typically washes out. The measured energy distribution thus provides a clear indication if an electronic transition to a dissociating state was involved or not. However, predissociation and tunneling have the same signature and one has to study the molecular structure to distinguish between these two. For example, it may be possible to differentiate between them if the final state(s) of the fragments is (are) different, so that the KER is related to a different asymptote, as shown in Fig. 2.

In the case of decay by an electronic transition to a lower dissociating state [process (c) in Fig. 2] a simultaneous measurement of the KER and the decay rate provides an experimental value of the transition rate as a function of internuclear distance, as the KER can be traced back to this coordinate. Tunneling decay rates [process (b) in Fig. 2], on the other hand, are very sensitive probes of the accuracy of structure calculations. This can be seen from the WKB formula for the tunneling rate,

$$\tau^{-1} \propto \exp\left(2\sqrt{2\mu} \int_a^b dR \sqrt{V(R) - E_{vl}} \right), \qquad (1)$$

where μ is the reduced mass of the molecule, a and b are the classical turning points, E_{vl} is the energy of the level vl, and $V(R)$ is the potential-energy curve. A small change in the potential-energy curve $V(R)$ results in a large change of the decay rate. Thus, measurements of decay rates provide a stringent test for theoretical treatments of molecular structure. However, for a direct comparison between the theory and experiment, the rovibrational state decaying by tunneling has to be identified. Here again, this can be achieved if both

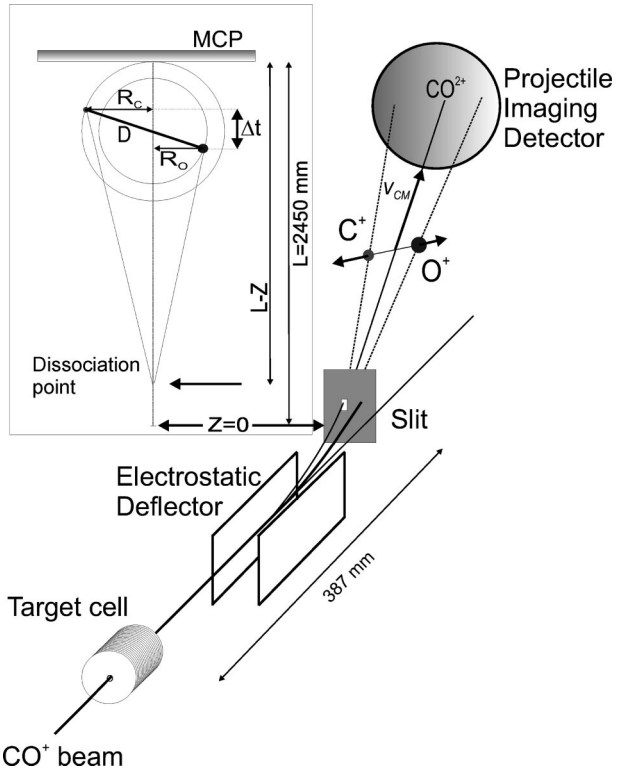

FIG. 3. Schematic view of experimental setup.

the lifetime and the KER are measured simultaneously, as shown schematically in Fig. 2.

Predissociation rates [process (a) in Fig. 2] are sensitive probes of the coupling between the curves, and the overlap between the initial and final vibrational wave functions. Measurements of such decay rates serve to test calculations of these coupling terms. Once more, a direct comparison with theory can be achieved only if the measured lifetime is state specific, i.e., the KER is measured simultaneously.

In the following section, we describe an experimental method where both the lifetime and KER are measured simultaneously for the unimolecular dissociation of doubly charged molecular ions.

III. METHOD

The basic idea of the simultaneous measurement of the lifetime and KER upon unimolecular dissociation of a long-lived state is to measure the distance between the dissociating fragments produced from fast (keV to MeV) molecular ions, a long distance from their dissociation point. The separation in space between the fragments is a function of both their kinetic energy in the center of mass frame and the elapsed time from when the molecular ion was formed. For simplicity, we will assume that the state decays by either tunneling or predissociation, in which case the KER has a unique value for a given initial quantum state.

The inset in Fig. 3 demonstrates the idea schematically. Assume that N_0 doubly charged molecular ions are produced at a distance L from the surface of a detector. If the molecular ions move at a constant velocity v_b in the direction of the detector, the number of molecules dissociating at a distance z is given by

$$N(z)dz = \frac{1}{v_b \tau} N_0 \exp(-z/v_b\tau)dz. \tag{2}$$

The distance D between the fragments upon hitting the surface of the detector, located at a distance $(L-z)$ from the dissociation point, is related to the KER E_k via

$$E_k = \frac{1}{2}\mu v^2 = \frac{E_b}{(L-z)^2}\left(\frac{m_A m_B}{(m_A+m_B)^2}\right)D^2, \tag{3}$$

where μ is the reduced mass of the molecule, m_A and m_B are the masses of the fragments, v is the relative velocity between the two fragments, and E_b is the beam energy. The relation between the distance D and the dissociation point z is given by

$$\frac{D}{v} = \frac{L-z}{v_b}. \tag{4}$$

Using probability conservation, one can relate the number of fragments hitting the detector separated by a distance between D and $D+dD$ to the number of molecules dissociating between z and $z+dz$:

$$N(z)dz = N(D)dD. \tag{5}$$

Thus, using Eqs. (2) and (4), we can obtain an explicit expression for $N(D)$:

$$N(D) = N(z)\left|\frac{dz}{dD}\right| = \frac{1}{v_b\tau}N_0 \exp\left(\frac{v_b D/v - L}{v_b\tau}\right)\frac{v_b}{v}$$
$$= \frac{N_0}{v\tau}\exp\left(\frac{D}{v\tau} - \frac{L}{v_b\tau}\right). \tag{6}$$

From Eq. (6), it can be seen that the distribution of distances between the two fragments depends directly on both the lifetime τ and the KER (through the fragment velocity v).

The distributions calculated for two metastable states with different KER's E_k and lifetimes τ are shown in Fig. 4. The chosen values are typical for what is expected from the unimolecular dissociation of CO^{2+}. The two states are clearly separated, and the thick line represent the superposition of these two states, assuming branching ratios of 90% and 10%, respectively. For these calculated spectra, the detector was located at a distance of 2450 mm from the origin, and the beam velocity was $v_b = 1.67$ mm/ns.

In order to measure the distance distribution $N(D)$, a multihit three-dimensional (3D) imaging detection system is needed. In the following, we describe the experimental setup, as well as the results obtained for the unimolecular dissociation of CO^{2+}.

IV. EXPERIMENTAL SETUP

Singly charged $^{12}C^{16}O^+$ molecular ions were produced in the rf ion source of the Technion 1-MV Van de Graaff accelerator from CO_2, and accelerated to 407 keV. The molecular ions were then directed by a 15° analyzing magnet toward a windowless gas (Ar) target cell where charge-stripping reactions took place, producing the $^{12}C^{16}O^{2+}$ ions.

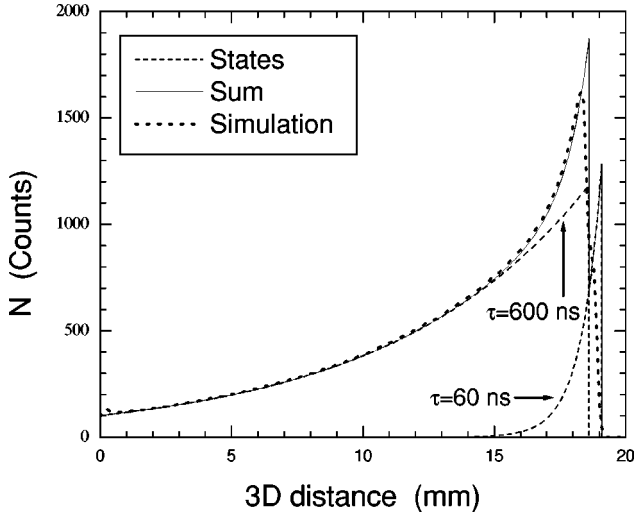

FIG. 4. Simulated three-dimensional (3D) spectrum of two states with δ function KER distributions. The parameters of the two states are $\tau=600$ ns and $E_k=5.7$ eV, $\tau=60$ ns and $E_k=6.0$ eV, with 90% and 10% populations, respectively. The simulation includes the convolution of the sum of these two states with the instrumental broadening (see text).

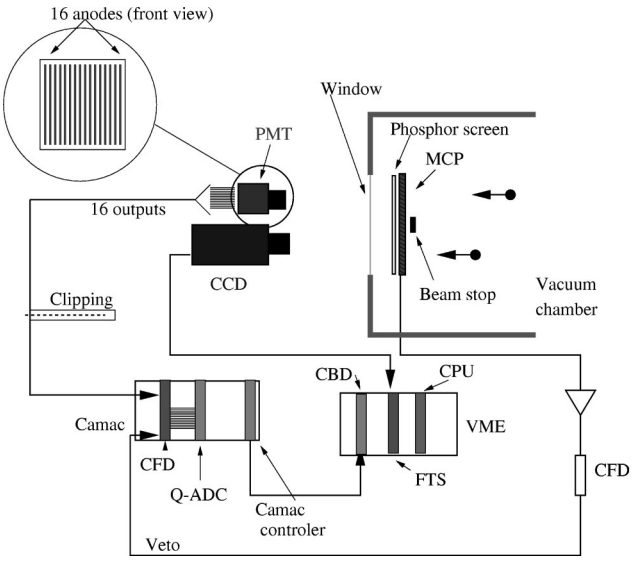

FIG. 5. Schematic view of the detection system. The electronic units used are: constant fraction discriminator (CFD), charge sensitive analog-to-digital converter (Q-ADC), camac branch driver (CBD), VERSAmodule Eurocard (VME), frame threshold suppressor (FTS).

A velocity selector was used before the target cell to direct only charged projectiles through and further clean the beam from any contaminants having a different velocity from the $^{12}C^{16}O^{+}$ beam. The pressure in the 3 mm long differentially pumped target cell was kept at 100 mTorr, while the pressure in the rest of the system was below 10^{-6} Torr. The reaction products emerging from the target cell were separated by an electrostatic parallel plate deflector. Details about these parts of the experimental setup and the experimental procedures are described in previous publications [13–15].

The $^{12}C^{16}O^{2+}$ dications were deflected by the electric field through a narrow vertical slit (0.73 mm wide) located 30 mm after the electrostatic deflector exit and directed toward a 40 mm diameter microchannel plate (MCP) detector placed 2450 mm downstream, as shown in Fig. 3. At this beam velocity, all C^{+} and O^{+} fragments of the dissociation are confined within the detection solid angle as long as the kinetic energy released upon dissociation is less than 21 eV, i.e., well above the expected 6–7 eV. The center of the detector was blocked by a 1.5 mm diameter disk positioned 266 mm in front of it in order to stop the nondissociated molecular fraction. As a result mostly ion pairs hit the detector, thus improving the efficiency of the measurement. The detection system consists of a MCP detector located in front of a phosphor screen anode. The phosphor screen was imaged via a charge-coupled device (CCD) camera in order to decode the positions of all hits, as shown in Fig. 5. The centroids of the light spots provide the x and y information for each detected ion, with an uncertainty of about 30 μm in both directions. The projection of the distance between the fragments onto the detector plane is defined as

$$d=\sqrt{(x_1-x_2)^2+(y_1-y_2)^2}, \tag{7}$$

later referred to as the two-dimensional distance. In Eq. (7), $x_{1,2}$ and $y_{1,2}$ are the x and y positions of each particle. To evaluate the component of the three-dimensional distance parallel to the beam direction, $v\Delta t$, the difference between the time of arrival of the two fragments, Δt, was measured. This time difference is up to 5 ns for a kinetic-energy release of 6 eV at the beam energy used. Thus a fast timing system with high resolution is essential for such measurements. In addition to the CCD camera, the phosphor anode was viewed by a 16 wire anode photomultiplier tube (PMT), which produced the timing signals while maintaining the correlation with the position information. The correlation is kept by associating the poor one-dimensional resolution position information from the PMT with the more precise two-dimensional information from the CCD output. The timing resolution was about 0.31 ns for $\delta(\Delta t)$, where $\Delta t=t_1-t_2$. The relative error in Δt is much larger than that of the two-dimensional distance, δd, and thus it dominated the uncertainty of our measurements. The three-dimensional distance between the fragments is given by

$$D=\sqrt{(v\Delta t)^2+d^2}. \tag{8}$$

To reduce random coincidences the phosphor screen voltage was turned off 60 ns after the first hit, using a photodiode to provide the trigger signal, and turned back on once data processing was done. A detailed description of this multiparticle three-dimensional imaging detector can be found in Ref. [16].

In addition to $C^{+}+O^{+}$ ion pairs from unimolecular dissociation of $^{12}C^{16}O^{2+}$, $N^{+}+N^{+}$ ion pairs from the dissociation of $^{14}N_2{}^{2+}$ were also detected. This is due to the presence of a small contaminant beam of $^{14}N_2{}^{+}$, molecular ions with the same mass over charge ratio and velocity as the main $^{12}C^{16}O^{+}$ beam. Furthermore, even if the $^{14}N_2{}^{2+}$ dissociates immediately after formation in the target cell, both N^{+}

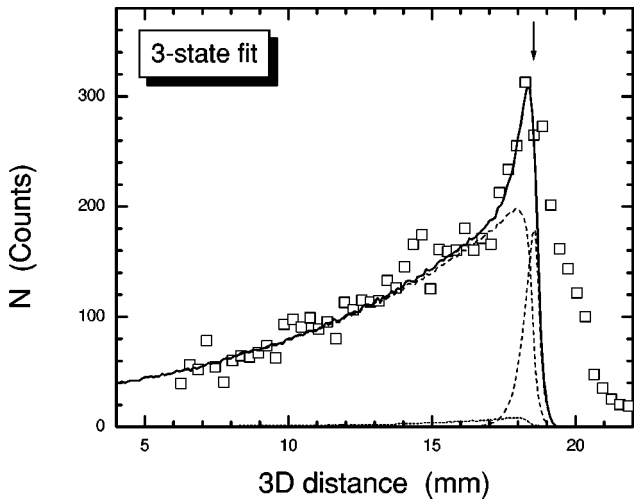

FIG. 6. Three-dimensional spectrum of $^{12}C^{16}O^{2+}$. The line is a three-state best fit to the data, with (1) $E_{k_1}=5.713$ eV, $\tau_1=680$ ns, and $N_1=2375$; (2) $E_{k_2}=5.841$ eV, $\tau_2=26$ ns, and $N_2=160$; (3) $E_{k_3}=5.655$ eV, $\tau_3=320$ ns, and $N_3=50$. Note that the KER values are not free parameters but are taken from Ref. [10] (see text for details).

fragments will be deflected along the same trajectory as the $^{14}N_2{}^{2+}$ dication, because they all have the same energy to charge ratio. Thus, even a minute fraction of $^{14}N_2{}^{+}$ relative to the $^{12}C^{16}O^{+}$ beam will produce a noticeable rate of $N^+ + N^+$ ion pairs. It was possible to distinguish between the nitrogen and carbon-oxygen ion pairs as the two fragments have different distances from the molecule center of mass, which has to be within the beam spot. The carbon-oxygen ion pair has a ratio of 3 to 4 between their distances relative to the center of mass, while the nitrogen pairs have equal distances. True ion-pair events were distinguished from random multihits on the detector by constraining the center of mass of the two hits to a small beam spot [17]. In this sense, our data analysis is similar to the one done in KER measurements using three-dimensional imaging (see, for example, Bruijn and Los [18]).

V. RESULTS AND DISCUSSION

The yield of ion pairs as a function of their distance from each other is shown in Fig. 6. No data are shown for short distances because of the overlap with the competing $N^+ + N^+$ dissociation channel and random events. A simulation was used for the data analysis [based on Eq. (6)] to include all effects of detector resolution (which are different for the spatial and time coordinates).

From a comparison between Fig. 6 and Fig. 4, it is easy to observe that more than one vibrational state is decaying during the time of flight between the narrow slit and the detector. A rough estimate based on Eq. (6) suggests that the KER's measured in the present case are in the range of 5.5 to 6.6 eV. Such a range of energy is in agreement with the range of energies measured by Lundqvist *et al.* [10]. The upper limit for the lifetime (650 ns) can be obtained from the slope of the short distance side of the distribution shown in Fig. 6, while the lower limit (~ 10 ns) is related to the time of flight between the gas target and the defining slits (see Fig. 3), which is a distance of 387 mm.

A complete analysis of the KER spectrum shown in Fig. 6 should include a superposition of functions of the form given in Eq. (6) (convoluted with the experimental resolution). Each of these functions has three parameters to be defined from the fit: the number of ions N_0 in the state at $z=0$ (i.e., at the defining slit shown in Fig. 3), the KER E_k, and the lifetime τ. However, because of the large number of states present in this spectrum, and the limited resolution (due to the limited distance between the defining slit and the MCP detector), we have focused on the three states having mean lifetimes between 200 and 700 ns according to Penent *et al.* [12]. Our experiment is more sensitive to this range of decay times because of the similarity to the flight time through the system. To reduce the number of fit parameters we used the KER values reported by Lundqvist *et al.* [10] for these states, $E_k=5.713$, 5.655, and 5.841 eV. Using these values, we have fitted the KER spectrum up to $D=18.55$ mm (which corresponds to $E_k=5.841$ eV) using the mean lifetimes and the number of ions in each state as free parameters. The results shown as a full line in Fig. 6 yield a lifetime of 680 ± 60 ns for the state with $E_k=5.713$ eV, and a much shorter value of 26 ± 8 ns for the state with $E_k=5.841$ eV. The fitted number of ions in the state with $E_k=5.655$ eV was consistent with zero, thus suggesting that it is not populated significantly in comparison to the other two states in the charge-stripping collisions forming the CO^{2+}. Furthermore, the value of the mean lifetime of this state, 320 ± 220 ns, has no significant impact on the quality of the fit, and as a result it cannot be determined to better precision than the measurement of Penent *et al.* [12], who reported $\tau=200\pm 100$ ns for this state.

We repeated the fit with only the first two states having $E_k=5.713$ and 5.841 eV. The results shown as a full line in Fig. 7 yield similar values for the mean lifetimes and branching ratios as before with improved precision due to the reduced number of parameters. The values were $N_0=2410 \pm 90$ and $\tau=670\pm 54$ ns, and $N_0=160\pm 30$ and $\tau=26.3 \pm 5.1$ ns, respectively, for these two states (where the reported errors are two standard deviations). The experimental results obtained with the present method are consistent with the previous state-specific measurements of Lundqvist *et al.* [10] and Penent *et al.* [12], as shown in Table I.

No attempt was made to fit the high E_k side of the KER spectrum (i.e., $E_k>5.841$ eV), due to the large number of possible contributing states for which the resolution is insufficient. However, the measured distance distribution for $D>18.5$ mm in Fig. 7 is consistent with the range of energy releases as measured by Lundqvist *et al.* [10] (we show one such state as an example in Fig. 7). Furthermore, from the overall shape of the spectrum, it is certain that none of the additional states have lifetimes longer than 30 ns.

From the measured number of ions and the mean lifetime of each state it is possible to determine the relative population of the states following the charge-stripping collision $CO^+ + Ar \rightarrow CO^{2+}$ at 407 keV. Note that the measured N_0

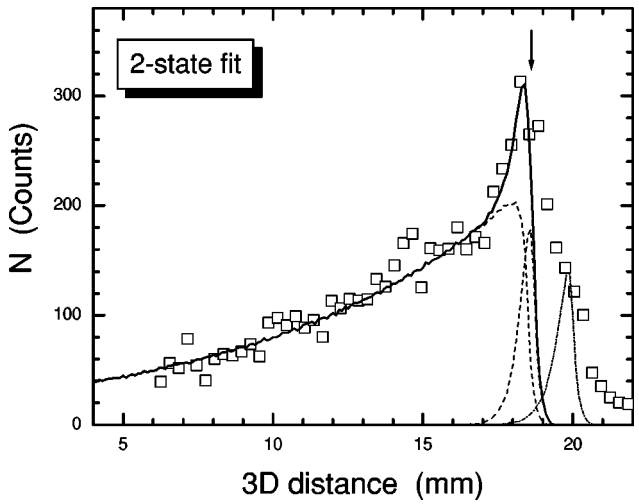

FIG. 7. Three-dimensional spectrum of $^{12}C^{16}O^{2+}$. The line is a two-state best fit to the data, with (1) $E_{k_1}=5.713$ eV, $\tau_1=670$ ns, and $N_1=2410$; (2) $E_{k_2}=5.841$ eV, $\tau_2=26$ ns, and $N_2=160$ (both shown as dashed lines). Note that the KER values are not free parameters of the fit (see text for details). In addition we show (dash-dotted line) the possible contribution of the $^1\Pi(v=5)$ state, for which Lundqvist *et al.* reported $E_k=6.71$ eV [10], $\tau=30$ ns, and $N_3=160$. A few additional vibrational states with mean lifetimes of the same order of magnitude will fill the large *D* region.

are related to the relative populations of the CO^{2+} states when these molecular ions reach the slit defining $z=0$ (see Fig. 3). The populations at the target cell were determined to be 3400 ± 160 and 10^6–10^7 for the states with KER's of 5.713 and 5.841 eV, respectively, i.e., the $^1\Sigma^+$ and $^1\Pi$ states, suggesting that the latter is populated more frequently than the former by a factor of more than 50. Furthermore, the data suggest that the $^3\Pi$ state is not significantly populated in these collisions. It is important to note that in our studies a removal of one electron was needed to produce the CO^{2+}, in contrast to the double ionization in the studies of Lundqvist *et al*. [10] and Penent *et al.* [12]; thus the relative populations are expected to be different. To populate the $^3\Pi$ state by charge-stripping a CO^+ molecular ion in its electronic ground state, the electron removed has to be a paired electron; in contrast, the singlet states $^1\Sigma^+$ and $^1\Pi$ are populated when the unpaired electron is removed. The suggested method thus also allows one to study the relative populations of long-lived states following charge-stripping collisions, or in other words the relative cross sections for these processes.

The measured mean lifetime of the state with $E_k=5.841$ eV, assigned to be the $^1\Pi(v=0)$ state, is much more precise than the previously reported values [10,12] (see Table I). In contrast, the previous measurements by Lundqvist *et al.* [10] and by Penent *et al.* [12] are superior in determining the energy of the dissociative states. They directly measure the KER in the first and the excitation energy in the second. Another advantage of the present technique is the wide range of lifetimes accessible by selecting the beam velocity such that the flight time through the system matches the mean lifetime one intends to measure.

In spite of the nice agreement between the measured energies and lifetimes also obtained for the state with $E_k=5.713$ eV, by Lundqvist *et al.* [10] and by Penent *et al.* [12] as well as with the present technique, the identity of this decaying state is still to be clarified. According to Lundqvist *et al.* [10] the measured state is $^1\Sigma^+(v=0)$ while Penent *et al.* [12] associated it with the next vibrational state, $^1\Sigma^+(v=1)$. The latter assignment is based on the nice agreement with the calculated vibrational levels bound to the potential-energy curves reported by Andersen *et al*. [7] and shown in Fig. 1.

To further probe this inconsistency it is useful to compare the measured mean lifetime to the theoretical prediction also, because this presents a sensitive test of theory, as discussed in Sec. I. This is due to the strong dependence of the mean lifetimes on the coupling between the states involved in the predissociation. Andersen *et al.* [7] computed potential-energy curves (PEC's) for the CO^{2+} system, but they presented the energies and mean lifetimes only for the resonances of the $^{13}C^{16}O^{2+}$ isotope. To compare our results on $^{12}C^{16}O^{2+}$ with theory we modeled the decay process, for the relevant reduced mass of the molecular ion, using the potential-energy curves and coupling from Andersen *et al.* [7], shown in Figs. 1(a) and 1(b), respectively. As discussed by Larsson *et al.* [20], the $^3\Pi$ ground state decays by direct predissociation due to its coupling to the repulsive $^3\Sigma^-$ state. $^1\Sigma^+$, on the other hand, decays by indirect predissociation, i.e., by its coupling to the $^3\Pi$ rather than by direct coupling to the repulsive $^3\Sigma^-$ state. To check the validity of our computational method, described briefly below for both direct and indirect predissociation, we first repeated the calculations for the $^{13}C^{16}O^{2+}$ isotope. We found reasonable agreement between our calculations and the more exact values reported by Andersen *et al.* [7] for this isotope (see Table

TABLE I. Measured mean lifetimes (in ns) of two states of $^{12}C^{16}O^{2+}$. The KER and excitation energy from the CO ground state for these states are as follows: (a) For the $^1\Pi(v=0)$ state, $E_k=5.841$ eV and $E_{exc}=41.818$ eV [10], and $E_{exc}=41.853$ eV [12]; (b) for the $^1\Sigma^+(v=0$ or 1) state (see text), $E_k=5.713$ eV and $E_{exc}=41.69$ eV [10], and $E_{exc}=41.725$ eV [12].

State	This work	Lundqvist *et al.* [11]	Penent *et al.* [12]	Field and Eland [6]	Safvan and Mathur [5]
$^1\Pi$	26 ± 5	<50	200^{+100}_{-200}		
$^1\Sigma^+$	670 ± 50	600 ± 100	700^{+200}_{-100}	600^{+600}_{-200}	1000 ± 250

TABLE II. Calculated mean lifetimes, KER's, and excitation energies of some states of CO^{2+}.

	$^{13}C^{16}O^{2+}$		$^{12}C^{16}O^{2+}$		
	τ(s)		τ(s)	KER (eV)	E_{exc} (eV)
State	Ref. [8]	This work	This work	This work	This work
$^3\Pi(v=0)$	2.0×10^{-2}	1.4×10^{-2}	0.72×10^{-2}	5.282	41.250
$^3\Pi(v=1)$	3.0×10^{-7}	2.9×10^{-7}	1.7×10^{-7}	5.451	41.419
$^3\Pi(v=2)$		4.2×10^{-10}	2.9×10^{-10}	5.614	41.582
$^1\Sigma(v=0)$	2.0×10^{-6}	0.81×10^{-6}	0.78×10^{-6}	5.512	41.480
$^1\Sigma(v=1)$	1.3×10^{-9}	0.78×10^{-9}	0.88×10^{-9}	5.745	41.713

II), suggesting that the approximations used here are adequate.

The energies as well as the wave functions of the vibrational levels bound to the $^3\Pi$ and $^1\Sigma^+$ states were calculated using the phase-amplitude method [19]. This method includes the shifts of the vibrational energy levels due to tunneling. Tunneling rates are negligible except for the highest excited vibrational states. Thus, our energy levels match nicely the previous values for both isotopes (see, for example, Refs. [7,12]).

The direct predissociation rate of any vibrational resonance bound in the $^3\Pi$ potential-energy curve was calculated by integrating over R the product of the vibrational wave functions and the electronic coupling between the two crossing states,

$$\frac{1}{\tau}=\Gamma \ \ (\text{a.u.})=2\pi\left|\int_0^\infty \psi_v(R)\psi_E(R)H^e(R)dR\right|^2, \qquad (9)$$

where

$$H^e(R)=\langle\phi_1(r,R)|H|\phi_2(r,R)\rangle \qquad (10)$$

is evaluated at an internuclear distance R, while ψ_v and ψ_E are the bound and continuum vibrational wave functions of the $^3\Pi$ and $^3\Sigma^-$ electronic states involved. Using the equation above is a better approximation for the predissociation rate than the commonly used expression evaluated at $\langle R\rangle$,

$$\frac{1}{\tau}=\Gamma \ \ (\text{a.u.})=2\pi|H^e(\langle R\rangle)|^2\langle\psi_v|\psi_E\rangle^2, \qquad (11)$$

because it takes into account better the dependence of the electronic coupling $H^e(R)$ on R (for a detailed discussion see Ref. [21]).

The $^1\Sigma^+$ state decays predominantly by indirect predissociation because of its mixing with the $^3\Pi$ state, which rapidly predissociates by spin-orbit coupling with the repulsive $^3\Sigma^-$ state. Indirect predissociation is affected by more than one vibrational level in the $^3\Pi$ state, and thus the width of each vibrational resonance bound to the $^1\Sigma^+$ state is given by

$$\frac{1}{\tau_{1,v_1}}=\Gamma_{1,v_1}(\text{a.u.})=2\pi\left[\sum_{v_j} a_{1,v_1;2,v_j}H_{2,v_j;3}\right]^2, \qquad (12)$$

where 1, 2, and 3 denote the $^1\Sigma^+$, $^3\Pi$, and $^3\Sigma^-$ states, respectively; the coupling between the intermediate and repulsive states $H_{2,v_j;3}$ is given by

$$H_{2,v_j;3}=\int_0^\infty \psi_{2,v_1}(R)H_{23}(R)\psi_{3,E}(R)dR; \qquad (13)$$

the mixing coefficients $a_{1,v_1;2,v_2}$ are given by the perturbation formula (if $H_{12}\ll\Delta E_{12}$)

$$a_{1,v_1;2,v_2}=\frac{H_{12}}{\Delta E_{12}}; \qquad (14)$$

and the coupling between the two bound states $H_{12}(R)$ is

$$H_{12}=\int_0^\infty \psi_{1,v_1}(R)H_{12}(R)\psi_{2,v_2}(R)dR. \qquad (15)$$

Note that $a_{1,v_1;2,v_j}$ and $H_{2,v_j;3}$ might be either positive or negative, thus resulting in accidental cancellation. For further details see Refs. [21] and [22].

For the electronic coupling $H^e(R)$, between the $^3\Pi$, $^1\Sigma^+$, and $^3\Sigma^-$ states we used the values calculated by Andersen *et al.* [7] [Fig. 1(b) here and Fig. 3 in their paper]. The wave functions of the vibrational resonances of the $^3\Pi$ and $^1\Sigma^+$ states were calculated using the phase-amplitude method. The continuum wave functions of the repulsive $^3\Sigma^-$ state were evaluated at the energy of the resonances using the same method. To calculate the indirect predissociation rate of any vibrational resonance bound to the $^1\Sigma^+$ state, the widths of all vibrational resonances of the $^3\Pi$ state were needed. The latter were calculated using Eq. (9). The calculated mean lifetimes, KER, and E_{exc} (excitation energy from the CO ground state) of a few low lying states are presented in Table II.

Now that we have calculated both the energy and the mean lifetime for each state of the $^{12}C^{16}O^{2+}$ isotope, they should both match for each vibrational state. For the state with a measured mean lifetime of 670 ns, for example, agreement with either energy or mean lifetime is possible, but not with both as required. It is important to note that the three independent measurements of this state, using different experimental techniques, are in good agreement with each other for the mean lifetime as well as for the energy of this state, even if previous work disagreed about the identity of the state [10,12]. Explicitly, the mean lifetime was measured

to be 600 ± 100 ns by Lundqvist *et al.* [10], 700^{+200}_{-100} ns by Penent *et al.* [12], and 670 ± 50 ns by us. These values are in good agreement with the calculated value of 780 ns for the $^1\Sigma^+(v=0)$ state, especially when one considers also the uncertainty in the calculated value, which is due to the approximation methods used. The uncertainty in the computed value, however, cannot account for differences of orders of magnitude that exist between the measured values and the computed value for the next vibrational state. The energy level of the state, measured either as KER [10] (and in this work) or as excitation energy from the CO ground state [12], was determined to be $E_k=5.713$ eV ($E_{exc}=41.69$ eV) by Lundqvist *et al.* [10] and $E_k=5.748$ eV ($E_{exc}=41.725$ eV) by Penent *et al.* [12]. The difference between these two high precision measurements is 35 meV, which is much smaller than the energy gap between the two lowest vibrational states of the $^1\Sigma^+$ state (see Table II). The measured energy is in good agreement with the calculated value for the $^1\Sigma^+(v=1)$ state and not with the ground vibrational state that agreed with the measured mean lifetime. In order to resolve this conflict between the experimental results and our calculations based on the available PEC's and coupling terms [7] we tried to shift the $^1\Sigma^+$ potential-energy curve upward relative to the $^3\Pi$, such that the energy of the $^1\Sigma^+(v=0)$ would match the measured value. This resulted in a mean lifetime for indirect predissociation of the $^1\Sigma^+(v=0)$ state that is two orders of magnitude too short in comparison to the measured value. The disagreement between the experimental results and the computed values might be due to the difficulties for theory to accurately predict the potential-energy curves of dications as discussed previously, for example, by Larsson [23].

There is a clear need for a more precise theoretical treatment of the CO^{2+} structure and decay. Such calculations can then be compared with the measured energy levels, which attained spectroscopic quality in recent years, as well as with the measured decay rates of specific states. The combined information on the state energy and decay rate provide a stringent test for such calculations, as demonstrated above. Future calculations might also provide possible state with mean lifetimes in the few seconds range, i.e., as long as those observed in storage rings [7,8].

VI. SUMMARY

The mean lifetimes of two states of $^{12}C^{16}O^{2+}$ were measured to be $\tau=670\pm50$ ns and $\tau=26\pm5$ ns for the states with $E_k=5.713$ eV and $E_k=5.841$ eV, respectively. The latter state is more likely to be populated in the charge-stripping reaction $CO^+ + Ar \rightarrow CO^{2+}$ at 407 keV by at least a factor of 50. A method for the simultaneous measurement of the mean lifetime and kinetic energy released upon dissociation, based on three-dimensional imaging of the dissociating fragments, was presented. The measured values reported in this paper are in good agreement with previous measurements [10,12] with improved precision on the mean lifetime measurement. The decay rates of a few low lying states of CO^{2+} by direct and indirect predissociation were calculated. The calculated mean lifetime of the $^1\Sigma^+(v=0)$ state is in good agreement with experiment but the energy of this state is too low in comparison with the measured value. On the other hand, the calculated energy of the $^1\Sigma^+(v=1)$ state is in good agreement with the experimental value but the calculated lifetime of this state is shorter than the measured value by orders of magnitude. There is a need for improved theoretical treatment of the CO^{2+} structure and decay rate.

ACKNOWLEDGMENTS

We wish to thank M. Larsson for providing the tabulated potential-energy curves of CO^{2+} from Ref. [7]. We are also grateful to F. Penent, Z. Herman, and M. Larsson for useful discussions. This work was supported in part by the Foundation for Promotion of Research at the Technion, in part by the Heinman Foundation at the Weizmann Institute of Science, and in part by the Division of Chemical Sciences, Geosciences and Biosciences Division, Office of Basic Energy Sciences, Office of Science, U.S. Department of Energy.

[1] D. Mathur, Phys. Rep. **225**, 193 (1993).
[2] A.S. Newton and A.F. Sciamanna, J. Chem. Phys. **53**, 132 (1970).
[3] R.G. Hirsch, R.J. Van Brunt, and W.D. Whitehead, Int. J. Mass Spectrom. Ion Phys. **17**, 335 (1975).
[4] G. Dujardin, L. Hellner, M. Hamdan, A.G. Brenton, B.J. Olsson, and M.J. Besnard-Ramage, J. Phys. B **23**, 1165 (1990).
[5] C.P. Safvan and D. Mathur, J. Phys. B **26**, L793 (1993).
[6] A. Field and J.H.D. Eland, Chem. Phys. Lett. **211**, 436 (1993).
[7] L.H. Andersen, J.H. Posthumus, O. Vahtras, H. Ågren, N. Elander, A. Nunez, A. Scrinzi, M. Natiello, and M. Larsson, Phys. Rev. Lett. **71**, 1812 (1993).
[8] D. Mathur, L.H. Andersen, P. Hvelplund, D. Kella, and C.P. Safvan, J. Phys. B **28**, 3415 (1995).
[9] G. Dawber, A.G. McConkey, L. Avaldi, M.A. MacDonald, G.C. King, and R.I. Hall, J. Phys. B **27**, 2191 (1994).
[10] M. Lundqvist, P. Bletzer, D. Edvarsson, L. Karlsson, and B. Wannberg, Phys. Rev. Lett. **75**, 1058 (1995).
[11] M. Hochlaf, R.I. Hall, F. Penent, H. Kjeldsen, P. Lablanquie, M. Lavollee, and J.H.D. Eland, Chem. Phys. **207**, 159 (1996).
[12] F. Penent, R.I. Hall, R. Panajotovic, J.H.D. Eland, G. Chaplier, and P. Lablanquie, Phys. Rev. Lett. **81**, 3619 (1998).
[13] I. Gertner, B. Rosner, and I. Ben-Itzhak, Nucl. Instrum. Methods Phys. Res. B **94**, 47 (1994).
[14] I. Ben-Itzhak, J.P. Bouhnik, I. Gertner, O. Heber, and B. Rosner, Nucl. Instrum. Methods Phys. Res. B **99**, 127 (1995).
[15] B. Rosner, I. Gertner, and I. Ben-Itzhak, in *Accelerator-Based Atomic Physics Techniques and Applications*, edited by S.M. Shafroth and J.C. Austin (AIP, Woodbury, NY, 1997), p. 509.
[16] Z. Amitay and D. Zajfman, Rev. Sci. Instrum. **68**, 1387 (1997).
[17] J. P. Bouhnik, Ph.D. thesis, Technion, 1998 (unpublished).
[18] D.P. Bruijn and J. Los, Rev. Sci. Instrum. **53**, 1020 (1982).

[19] E.Y. Sidky and I. Ben-Itzhak, Phys. Rev. A **60**, 3586 (1999).
[20] M. Larsson, B.J. Olsson, and P. Sigray, Chem. Phys. **139**, 457 (1989).
[21] H. Lefebvre-Brion and R.W. Field, *Perturbation in the Spectra of Diatomic Molecules* (Academic Press Inc., New York, 1986), Chap. 6.
[22] I. Kovács and A. Budó, J. Chem. Phys. **15**, 166 (1947).
[23] M. Larsson, Comments At. Mol. Phys. **29**, 39 (1993).